Journal of Alloys and Compounds 583 (2014) 578–586

Contents lists available at ScienceDirect

Journal of Alloys and Compounds

journal homepage: www.elsevier.com/locate/jalcom

Effect of manganese doping on the optical property and photocatalytic activity of nanocrystalline titania: Experimental and theoretical investigation

Susmita Paul, Pawan Chetri, Amarjyoti Choudhury *

Department of Physics, Tezpur University, Napaam 784028, India

ARTICLE INFO

Article history:
Received 7 May 2013
Received in revised form 22 July 2013
Accepted 30 August 2013
Available online 13 September 2013

Keywords:
Density functional theory (DFT)
Trap states
Photoluminescence
Photocatalytic activity

ABSTRACT

Nanocrystalline titania are doped with three different concentrations of manganese. The prepared nanoparticles have been characterized using different analytical techniques for analyzing their phase contents, nanocrystallite size distribution, band gap and photoluminescence. The changes in the property after doping are attributed to the introduction of Mn 3*d* states that act as electron trapping states .To further justify the creation of these trap states that has some strong correlation in contributing to enhanced photocatalytic activity, theoretical calculation based on density functional theory using VASP Software has been considered .The structure of undoped and manganese doped TiO_2 has been adapted to the minimum energy level configuration and corresponding calculation of density of states have indicated the state responsible for enhancement of photocatalytic activity.

1. Introduction

Photocatalytic degradation of organic pollutants with Titania (TiO_2) has received intense attention because of its low cost, high stability, and nontoxicity [1]. However the universal applications of TiO_2 is restricted by two primary factors: firstly its fast recombination of photo-generated electron/hole (e^-/h^+) pairs, secondly large band gap (3.2 eV) that makes it incapable for utilizing visible light. Therefore reducing the band gap of TiO_2 to make it photosensitive to visible region has been one of the major goals in photocatalytic applications. Several modifications have been suggested such as making composite with other oxide semiconductors [2,3], sensitizing TiO_2 with low band gap semiconductors such as CdS [4] and doping with metals and non-metals such as C, N, S, Ni [5–7]. Dopant ion incorporation is expected to induce shallow donor or acceptor states for effective ionization under photon illumination, leading to prolonged carrier diffusion length before they are combined and thereby offers better photocatalytic activity [8]. However photocatalytic activity of some photocatalysts did not improve despite observable red shift, as the doping induced defect states act as recombination centers when the charge carriers migrate from inside of the photocatalyst to the surface [9].

Unlike most of the 3*d* transition metal ion dopant, manganese doped TiO_2 has generated considerable interests as a photocatalyst showing optical response in the visible region and as oxide based dilute magnetic semiconductor showing ferromagnetism at room temperature [10–12]. In this work we have attempted to report the effectiveness of manganese doped TiO_2 nanoparticles in photocatalytic degradation of phenol under visible light. The phase structure and particle size of the prepared nanoparticles are characterized by XRD, RAMAN and HRTEM. XPS spectra is studied to analyze the dopant state and oxygen vacancy. Photoluminescence spectroscopy and time resolved photoluminescence spectroscopy are applied to study the recombination process of the photogenerated charge carriers that are affected by the incorporation of Mn 3*d* states. Based on the experimental results theoretical calculations based on density functional theory are carried out to further establish the presence of *d*-states.

2. Experimental methods

2.1. Synthesis method

Mn^{2+} doped TiO_2 nanoparticles with three different concentrations (3%, 5%, 7%) were synthesized via sol–gel method. The precursor for dopant and host precursors were manganese acetate tetrahydrate and titanium iso-propoxide respectively. 5 ml of Titanium Isopropoxide and 15 ml of 2 propanol were added to a 100 ml conical flask under constant stirring, followed by the addition of 1 ml of water to initiate the hydrolysis reaction. When a white thick solution was formed the dopant precursor solution was added and stirred for 7–8 h. During such process first a sol was formed which ultimately transformed into a gel. The gel was then centrifuged in water followed by ethanol for 4 times. The centrifuged product was dried at 80 °C. The resulting product was finally annealed at 450 °C to obtain crystalline manganese doped anatase TiO_2 nanoparticles.

* Corresponding author. Tel.: +91 3712267120; fax: +91 371222345.
E-mail address: ajc@tezu.ernet.in (A. Choudhury).

0925-8388/$ - see front matter © 2013 Elsevier B.V. All rights reserved.
http://dx.doi.org/10.1016/j.jallcom.2013.08.209

2.2. Characterization and measurements

The structure of all the samples are determined using Rigaku Miniflex CD 10041 XRD unit with copper target and λ = 1.54 angstrom at a scanning rate of 1°/min and in the scanning range of 10–80°. High resolution transmission electron microscope images for morphology and particle size determination are observed with JEM-2100, 200 kV JEOL. Raman spectra of the samples are acquired with Reinshaw in via Spectrometer. The 514.5 nm emission of Argon-ion laser is used as the excitation source. To study the composition of photocatalysts X-ray photoelectron spectroscopy (XPS) is recorded on KRATOS-AXIS 165 instrument equipped with dual aluminium–magnesium anodes using the Mg K radiation ($h\nu$ = 1253.6 eV) operated at 5 kV and 15 mA with pass energy 80 eV and an increment of 0.1 eV .The samples were degassed out for several hours in XPS chamber to minimize air contamination to sample surface. The fitting of the XPS curve have been done using a non-linear square method with the convolution of Lorentzian and Gaussian functions after a polynomial background was subtracted from the raw spectra. Diffuse Reflectance Spectra (DRS) of all the samples are taken with Shimadzu-2450 UV–Vis spectrometer. The photoluminescence (PL) measurements at room temperature are recorded with PERKIN ELMER LS 55 fluorescence spectroscopy. Time resolved photoluminescence spectra (TRPL) are recorded on a IBH Horiba-Yvon TCSPC using 340 nm NanoLED (FWHM = 750 ps) and 375 nm NanoLED (FWHM = 300 ps) as excitation source for the samples with a time scale of 0.007 ns/channel.

2.3. Computational detail

A 2 × 2 × 1 supercell is built with the unit cell of TiO_2 in anatase form. The undoped supercell contains 16 atoms of Ti and 32 atoms of oxygen which gives $Ti_{16}O_{32}$ (Fig. 1a). The Mn doped TiO_2 takes the form as $Ti_{15}MnO_{32}$ (Fig. 1b). The minimum energy state is computed by varying the internal position of atoms until the residual force is 0.01 eV/A^0. The cutoff kinetic energy for the structural optimization is set to 400 eV along with the convergence criterion of 10^{-5} eV. A 3 × 3 × 3 K-mesh is used which correspond to spacing less than $0.3(A^0)^{-1}$ in reciprocal space to calculate density of states (DOS) and band structure; Fermi level is considered to be at 0 eV. The effect of manganese (Mn) on the TiO_2 system is understood by substituting one center titanium (Ti) atom by Mn atom and allowing it to relax in all directions. We performed density functional calculations using generalized gradient approximation (GGA) with Perdew–Burke–Ernzerhof (PBE) to describe the electron–electron exchange and correlation effects. The density functional theory (DFT) equations are solved via projector augmented wave (PAW) method as implemented in Vienna Ab Initio Simulation Package (VASP) and interfaced with MedeA technology platform.

2.4. Photocatalytic activity

Photocatalytic activity for the undoped and manganese doped TiO_2 nanoparticles were studied by examining the degradation of aqueous solution of phenol. For visible light irradiation a 25 watt white lamp was used. In order to carry out the process 50 mg of the photocatalyst was added to 50 ml water in a 100 ml beaker. To it 5 mg of phenol was added and the solution was stirred for about half an hour to obtain the absorption–desorption equilibrium. The catalyst loaded phenol solution was then irradiated for 20, 40, 60, 80 min. After completion of the irradiation process the samples was centrifuged at 10,000 rpm to make it free from any catalyst. 5 ml of the aliquot was taken to measure the absorbance. The degradation efficiency was calculated by using the equation:

$$\%D = C/C_o \times 100 \quad (1)$$

C_o is the initial concentration and C is concentration after time t.

3. Results and discussions

3.1. Structural and morphological study

The XRD patterns of $Ti_{1-x}Mn_xO_2$ (x = 0.03, 0.05, 0.07) are shown in Fig. 2. Data estimated from the analysis of these diffractograms are tabulated in Table 1. All the diffraction peaks are well indexed to the tetragonal anatase phase structure (JCPDS-782486) and no hint of manganese containing phases is resolved. The main anatase peak (101) shifts to lower angles with increase in manganese concentration (inset of Fig. 2). Further an increase of the lattice c-parameter, cell volume and strain is noticed (Fig. 3 and Table 1). The observed trend in particular specifies introduction of manganese ions in the lattice and somewhat correlates with the observation on anatase titania doped with other transition metal ions [13]. The average crystallite size are calculated by using the Debye Scherrer's formula $d = \frac{0.9\lambda}{\beta Cos\theta}$ where λ is the wavelength of the X-ray source used; β is the full width at half maximum (FWHM); θ is the bragg diffraction angle and the dependence of grain size on manganese incorporation is depicted in Table 1. As can be seen from the XRD patterns (inset of Fig. 1), the diffraction peak (101) gets broadened as the manganese concentration is increased suggesting a systematic decrease in grain size. For undoped TiO_2 the average grain size is 18 nm (fwhm = 0.4308 radian) while it decreases to 7 nm (fwhm = 1.168) with 7% manganese incorporation. The incorporated manganese ions in the TiO_2 lattice thus suppress the grain growth by interfering into the intergranules that inhibit the grain boundary mobility or alter the surface energy leading to a decrease in grain growth velocity or nucleation energy obstruction resulting in decrease in grain size [14,15].

Fig. 4a and b shows the transmission electron microscopic images of undoped and 5% Mn doped TiO_2 nanoparticles. The average particle size for undoped titania is 21 nm while it decreases to 10 nm for 5% manganese doping concentration.

The effect of manganese doping on the microstructural change in nanocrystalline titania is further studied by Raman Spectroscopy, Fig. 5. Anatase TiO_2 has six active Raman modes ($A_{1g} + 2B_{1g} + 3E_g$) [16]. The intense E_g peak appears at 148 cm^{-1}. The other E_g peak at 199 and 642 cm^{-1}. One B_{1g} peak appears at 398 cm^{-1} and the ($A_{1g} + B_{1g}$) peak appears at 520 cm^{-1}. Compared to pure one the most intense E_g Raman peak at 146 cm^{-1} in manganese doped TiO_2 exhibits a decrease in intensity and blue

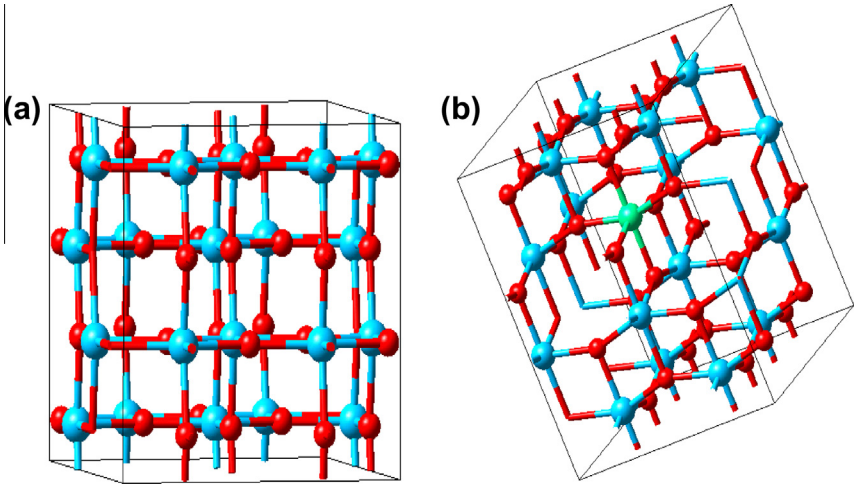

Fig. 1. (a) 48 Atoms supercell of TiO_2 and (b) Mn substituted 48 atoms supercell of TiO_2.